minerals

MDPI

Article

Study on the Nonlinear Characteristics of EMR and AE during Coal Splitting Tests

Liming Qiu [1,2,3,4], Yi Zhu [1,2], Dazhao Song [1,2,3,*], Xueqiu He [1,2], Weixiang Wang [5], Yang Liu [1,2], Yuzhe Xiao [1,2], Menghan Wei [1,2], Shan Yin [1,2] and Qiang Liu [1,2]

1 State Key Laboratory of the Ministry of Education of China for High-Efficient Mining and Safety of Metal Mines, University of Science and Technology Beijing, Beijing 100083, China; qiulm@ustb.edu.cn (L.Q.); zhuyi980315@163.com (Y.Z.); hexq@ustb.edu.cn (X.H.); 18810571557@163.com (Y.L.); xyz1037236113@126.com (Y.X.); weimh626@163.com (M.W.); ysviola@163.com (S.Y.); g20208081@xs.ustb.edu.cn (Q.L.)
2 School of Civil and Resources Engineering, University of Science and Technology Beijing, Beijing 100083, China
3 State Key Laboratory Cultivation Base for Gas Geology and Gas Control, Henan Polytechnic University, Jiaozuo 454003, China
4 State Key Laboratory of Coking Coal Exploitation and Comprehensive Utilization, Pingdingshan 467099, China
5 BGRIMM Technology Group, Beijing 102628, China; wangweixiang@bgrimm.com
* Correspondence: song.dz@163.com; Tel.: +86-18515139977

Abstract: Coal and rock dynamic disasters have been the main concern in underground engineering because these seriously threaten the safety of miners and industrial production. Aiming to improve the EMR and AE monitoring technology, the refined nonlinear characteristics of EMR and AE during coal splitting failure are studied using Hilbert-H and multifractal theory, and valuable information pertaining to coal fracture law contained in EMR and AE waveform was revealed. The results show that the EMR and AE of coal splitting failure are related to the process of coal crack propagation. They possess the same initiation time and frequency band, however, the signal duration of EMR is comparatively longer than AE, and the main frequency of AE is higher than EMR. The EMR of coal splitting failure has the same excitation source as AE; nonetheless, the excited forms display different behavior. In terms of signal duration, the distribution of EMR signal is relatively uniform, the proportion of large-signal is less, the amount of information is more than that of AE, and the multifractal characteristics are more complicated. During the coal splitting failure, AE is mainly generated in the process of wall vibration caused by crack propagation, while the generation of EMR includes piezoelectric effect, charge separation, free charge vibration, charge neutralization and other processes, making EMR more complicated than AE and has a relatively low frequency. The research provides an effective method for studying nonlinear refinement characteristics of coal EMR and AE, and can provide an important basis for the study of the mechanism of EMR generation.

Keywords: electromagnetic radiation; acoustic emission; nonlinear characteristics; Hilbert-Huang transform; multifractal

Citation: Qiu, L.; Zhu, Y.; Song, D.; He, X.; Wang, W.; Liu, Y.; Xiao, Y.; Wei, M.; Yin, S.; Liu, Q. Study on the Nonlinear Characteristics of EMR and AE during Coal Splitting Tests. *Minerals* **2022**, *12*, 108. https://doi.org/10.3390/min12020108

Academic Editors: David Cliff, Anye Cao and Zhenlei Li

Received: 5 December 2021
Accepted: 17 January 2022
Published: 19 January 2022

1. Introduction

The deep earth comprises huge energy resources that ultimately contribute towards economic significance. In this context, exploring and researching the deep earth has become an important concern for China's scientific and technological innovation [1]. However, with the increase of mining depth and mining intensity of coal and other resources, the stope structure is increasingly becoming complex, resulting in frequent disasters such as rock burst. These disasters generally lead to severe vibration, deformation or collapse damage of the roadway, failure or instantaneous destruction of the support system, resulting in displacement, overturning, damage of production facilities and casualties in the roadway,

which seriously threatens the safety of miners and industrial production [2–5]. Such disasters have resulted in worldwide casualties and economic losses in the past. For example, on 27 November 2017, a coal mine in Minbu Town, Magway Province, Myanmar collapsed, killing eight people. On 11 September 2020, a gold mine in Kamituga City, South Kivu province, Congo collapsed, killing more than 50 people. On 4 November 2020, a coal and gas outburst accident occurred in a coal mine in Tongchuan City, Shaanxi Province, China, killing eight people.

Accurate and effective monitoring is an important guarantee for preventing dynamic disasters. With the joint efforts of worldwide researchers, various coal and rock dynamic disaster prediction indicators have been put forward. However, at present, the prevention and control of mine rock bursts and other disasters is still demanding [6]. In the process of coal rock failure, elastic wave, electromagnetic radiation (EMR) and charge release are accompanied [7–10]. Among them, EMR is a type of energy released in the form of an electromagnetic wave during the deformation and fracture of coal and rock under load. EMR monitoring technology has been proved to be an effective nondestructive testing method, used to monitor the whole failure process of rock from micro cracks to macro failures under loading. Compared with other geotechnical engineering measurement methods, electromagnetism has the advantages of directionality, no contact and continuous monitoring. At present, it has been widely used in mine coal and rock dynamic disaster monitoring [11]. Frid et al. [12] studied the electromagnetic signal characteristics caused by rock crack propagation and proposed a disaster prediction method based on the number of electromagnetic pulses of coal rock fracture. He et al. [13] developed mine EMR monitoring equipment for dynamic monitoring rock burst hazard in the coal mining face. Lichtenberger et al. [14] considered that the intensity of the EMR pulse is directly proportional to the shear stress and evaluated the direction of the maximum principal stress in the tunnel through the developed monitoring equipment. Qiu et al. [15] used the positive correlation between the stress state of coal and rock and electromagnetism to monitor coal and gas outburst, considering that the electromagnetic intensity in the risk area of coal and gas outburst was high, and considering that the sudden increase of electromagnetism was the precursor of the outburst. Gade et al. [16] studied the acoustic and electrical phenomena during the fracture of epoxy resin materials and explored the determination of the crack surface direction of carbon fiber reinforced polymer materials by EMR. Greiling et al. [17] studied the relationship between EMR and the direction of formation principal stress, and considered that the direction of EMR is parallel or perpendicular to the crack surface. Furthermore, on this basis, a method to determine the formation shear zone by using EMR is proposed.

Studying the generation mechanism of EMR from coal and rock is the basis of the application of this technology. Previously, extensive research has been done on the electromagnetic response mechanism of coal and rock under load, achieving fruitful results, and defining various EMR mechanisms. Ogawa et al. [18] believed that the walls on both sides of the new surface during rock failure have different electrical charges, and the crack propagation process was equivalent to the charge and discharge process of a dipole; therefore, electromagnetism signals outward. Cress et al. [19] believed that the rotation and vibration of newly charged fragments during rock failure could stimulate low-frequency electromagnetic signals. Zhu et al. [20] believed that the electromagnetic signals in the process of rock failure were generated by the accelerated movement of the charge at the crack tip with the crack propagation. Rabinovitch et al. [21] conducted experimental research on the stage characteristics of low-frequency electromagnetic signals in the process of coal and rock failure. They proposed a model of electromagnetic signals excited by dipole oscillation at the crack tip. Pan et al. [22] believed that the crack propagation caused by tensile stress in the process of tensile failure of coal and rock, resulting in damage localization, was one of the critical reasons for the generation of free charge. Han et al. [23] studied the electromagnetic effect of rock under high stress and considered that the complex changes of the electromagnetic signal spectrum and amplitude in different failure stages were caused

by different types of electric dipole produced by crack propagation. It is evident from the earlier studies that the electromagnetic response mechanism of coal rock failure is generally related to the crack propagation during loading. However, to the best of the author's knowledge, none of these studies focused on the charge movement and excitement of the electromagnetic signal.

Acoustic emission (AE) can also be induced during crack propagation. In the general case, AE may occur during the deformation and fracture process of the coal in two situations—growth and propagation of new cracks, and friction and collision between cracks—and the AE activity will be larger and more concentrated during the fracture [24].

Interestingly, it was found that in the process of coal and rock destruction, AE often appears simultaneously with EMR [6,25–28]. Therefore, many scholars have researched the relationship between them. Wang et al. [26] found that the EMR and AE of coal and rock increased with stress and decrease with the decreased of stress. Sa et al. [27] found that the EMR of coal and rock has a memory effect different from the Kaiser effect of AE. They believed that the EMR is related to the generation and propagation of cracks and is a comprehensive reflection of coal and rock's damage, deformation, and damage degree. Zhang [28] believed that AE and EMR did not belong to synchronous signals—AE is directly related to crack development, while EMR is an indirect product of crack development.

Previous research has shown that in the process of coal fracture, EMR and AE always appear simultaneously. Their generation is closely related to crack propagation. The intensity of crack vibration determines the intensity of EMR and AE. The two technologies are often used in conjunction with coal mine disaster monitoring. Since AE is a mechanical wave, it can directly characterize the crack propagation process. The simultaneous use of EMR and AE is conducive to revealing the refinement process of coal failure. However, most of the past research mainly focused on the time series of the characteristic parameters of EMR and AE, such as events rate, events amplitude, intensity and pulse, and less on the waveform characteristics. In fact, both EMR and AE signals exist in the form of waves, with obvious nonlinear characteristics. At present, the nonlinear characteristics of EMR and AE waveform are not still in-depth researched; subsequently, the correlations and differences of their fine characteristics, which hold an imperative meaning for clarifying the relationship between coal and rock EMR and fracture and revealing the mechanism of EMR generation, are also rarely reported.

With the above motives, this paper intends to study the fine characteristics of EMR during coal splitting failure by Hilbert Huang Transformation and multi-fractal theory, and to compare with those of AE to reveal the correlation and difference between the two signals. On this basis, the excitation mechanism of electromagnetic radiation in the process of coal splitting failure is studied. The research results have theoretical value for the application of EMR and AE monitoring technology.

2. Experimental Scheme and Data Processing Method

2.1. Experimental System and Test Scheme

The schematic diagram of the coal load failure force acoustic–electric experimental system is shown in Figure 1. The system consists of an electromagnetic shielding system, a loading and control system, an acoustic and electrical data acquisition system, etc. Among these, the comprehensive shielding efficiency of the shielding room is 75 dB, which can effectively reduce the interference of external electromagnetic field to the experimental results. YAW-600 type testing machine (Jilin Guangteng Automation Technology Co., Ltd., Changchun, China)is used as a loading system, the load resolution of which is 3 N and the displacement resolution is 0.3 μm. The acoustic and electrical data acquisition system is composed of SAS-560 type EMR ring antenna (Changzhou Leining Electromagnetic Shielding Equipment Co., Ltd, Changzhou, China), common AE sensor, signal amplifier, data acquisition instrument, data processing host, etc. Various sensors are connected to the same acquisition instrument to ensure the synchronization of data transmission. The high-speed data acquisition instrument has 12 data acquisition channels, synchronous

signal trigger, maximum acquisition frequency of 10 MHz, A/D conversion accuracy of 16 bits, and input signal voltage range of ±5 V. The EMR ring is placed facing the sample, keeping a distance of about 5 cm parallel to the grinding plane of the sample. The response frequency range of the EMR antenna is 20 Hz~2 MHz, and the response is stable in the range of 20 Hz~200 kHz. The amplification factor of the amplifier is 40 dB, and the input and output impedance is 50 Ω. The response frequency of the AE sensor is 50 Hz~400 kHz, and the response is stable in the range of 50 Hz~200 kHz. The amplification factor of the amplifier is 40 dB, the input impedance is >10 MΩ and the output impedance is 50 Ω. EMR and AE signals analyzed in the work are the data after analog-to-digital conversion and amplification of original signals, characterized by the sensor's voltage value. The measurement of the electromagnetic field tests the change of magnetic flux. As shown in Figure 1, we use the induction coil to test the EMR signal generated by coal fracture. The electromagnetic field is measured in the horizontal direction. The acoustic and electrical data acquisition systems are located outside the shielding room. After loading, the coal fracture signal is received by the EMR antenna and AE sensor, amplified by the amplifier and transmitted to the acquisition system in the form of a digital signal for later analysis on the host.

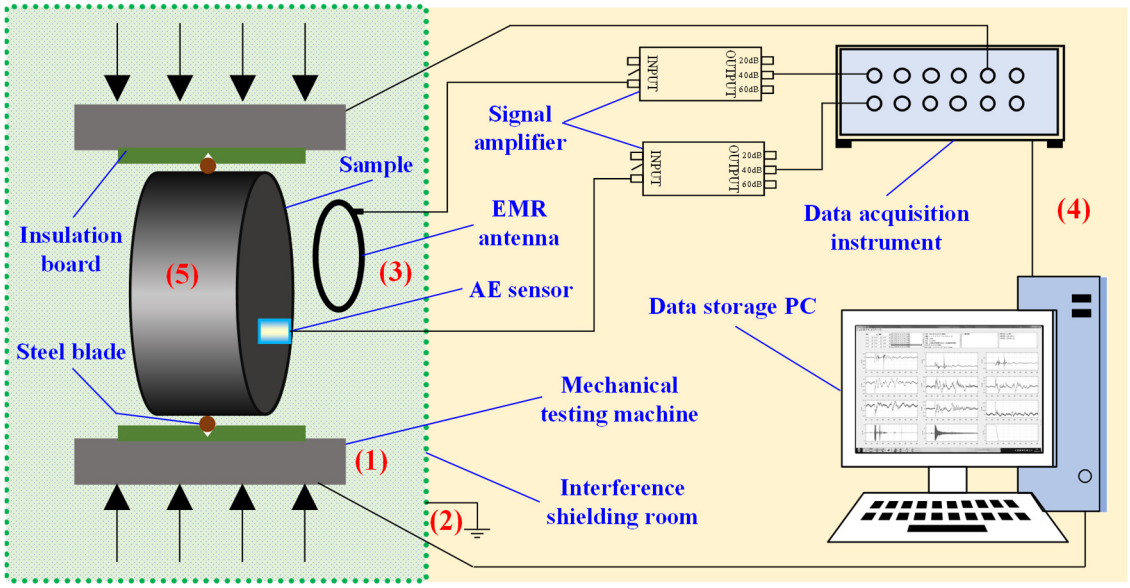

Figure 1. Schematic diagram of the experimental system. (1) Loading control system, (2) Interference shielding system, (3) Acoustic and electrical signal monitoring system, (4) Data acquisition system, (5) Sample.

2.2. Test Scheme

In this study, the coal sample used in the experiment was acquired from a coal mine in Shanxi Province, China. Firstly, a large coal sample was obtained, then coring, cutting and grinding were carried out to make a splitting sample with the size of ϕ 50 mm × 25 mm, the number of samples is 20, and the flatness of the end face of the sample shall be controlled within ±0.02 mm.

During the loading process of the splitting method, the upper and lower blades of the fixture are in contact with the sample. Under the load, the stress concentration occurs at the contact position between the upper and lower blades and the sample. When the concentrated stress exceeds the bearing limit of the coal rock sample, the sample is split by the blade. During splitting failure, the final collapse of the specimen usually shapes one fracture plane from the top to the bottom of the specimen, it is easier to obtain a relatively isolated signal than uniaxial compression experiment. This is also the reason why we take splitting experiments.

Before the experiment, set the sampling frequency of EMR and AE to 2 MHz to ensure sufficient resolution, and set the amplifiers of EMR and AE to 40 dB amplification.

Then, set the load parameters, apply 0.5 kN preload to the coal sample to ensure full contact between the blade and the sample, adopt the displacement control, and set the loading rate of 5 μm/s.

After ensuring that the experimental wiring was accurate and debugging was correct, we closed the door of the EMR shielding room and turned on the data acquisition system and the press of the acquisition instrument. After the data were stable, we recorded the data of EMR and AE.

After the sample broke, we stopped loading and saved the data for subsequent analysis.

2.3. Nonlinear Characteristic Analysis Method of Waveform

2.3.1. Analysis Method of Time-Frequency Fine Characteristics of the Waveform

At present, the main frequency analysis method is the Fourier transform. The amplitude-frequency spectrum of the EMR waveform can be obtained by Formula (1). In addition, based on Fourier transform, fast Fourier transform and other methods are developed [26].

$$F(\omega) = \int_{-\infty}^{\infty} f(t)e^{-i\omega t}\mathrm{d}t \tag{1}$$

In practical applications, the Fourier transform is usually mainly suitable for nearly stationary signals, and it is impossible to extract the time-frequency characteristics of signals simultaneously. Moreover, the time resolution and frequency resolution of the Fourier transform are the same in the global range. The area of each time-frequency window is fixed, resulting in its time-frequency resolution not being very high at the same time.

In order to improve the resolution of nonlinear signal analysis in the time and frequency domain, scholars proposed the empirical mode decomposition method. This method first carries out empirical mode decomposition (EMD) and then Hilbert spectrum analysis. Firstly, the given signal is decomposed into several intrinsic mode functions (intrinsic mode functions IMF) by the EMD method. Then, each IMF is represented in the joint time-frequency domain by the Hilbert transform. Finally, the Hilbert spectrum of the original signal will be obtained by summing the Hilbert spectrum of all IMF. Compared with traditional signal or data processing methods, HHT can analyze nonlinear and non-stationary signals, and achieve high accuracy in time and frequency at the same time.

Assuming that the original waveform signal is a sequence, then the sequence can be represented by multiple components and a mean value [29]:

$$x(t) = \sum_{i=1}^{n} c_i(t) + r_n(t) \tag{2}$$

where $c_i(t)$ is the i-th component and $r_n(t)$ is the n-th residuum of $x(t)$.

According to the amplitude function and instantaneous frequency, the original EMR waveform signal can be expressed as:

$$x(t) = Re\sum_{i=1}^{n} A_i(t)e^{j\int \omega_i(t)dt} \tag{3}$$

The Hilbert transform of the IMF of each order is obtained by decomposing the EMR waveform signal, and the distribution of the signal amplitude on the plane of time and frequency is called Hilbert time spectrum, which can be expressed as:

$$H(\omega, t) = Re\sum_{i=1}^{n} A_i(t)e^{j\int \omega_i(t)dt} \tag{4}$$

By integrating the amplitude of the above Hilbert spectrum with time, the Hilbert energy spectrum and Hilbert instantaneous energy spectrum can be obtained as follows [29]:

$$E(\omega) = \int_0^T H^2(\omega, t)dt \tag{5}$$

$$IE(t) = \int_\omega H^2(\omega, t)d\omega \tag{6}$$

Equations (5) and (6), respectively, describe the energy of each unit frequency on the full-time domain and the accumulation of all frequency energy in unit time, showing the change of EMR energy with time.

EMR and AE excited during coal failure are transient non-stationary random signals [30]. Moreover, the spectral composition of these two waves is complicated and there are many influencing factors. It is difficult to fully reveal their time-frequency characteristics by using ordinary spectrum analysis methods. HHT transformation can be well used in the analysis of EMR waveform and AE waveform with nonlinear and non-stationary characteristics, and can extract the primary characteristic information of the time history curve.

2.3.2. Analysis Method of Fractal Characteristics of the Waveform

The fractal dimension is used to describe unstable signals and objects. It is an effective tool to describe complicated and unstable signals.

For a time-series $x(t)$, when calculating the multifractal dimension and multifractal spectrum, a partition function $X_q(\delta)$ is defined first [30],

$$X_q(\delta) = \sum P_i(\delta)^q = \delta^{\tau(q)} \tag{7}$$

where τ (q) is the quality index, and q is the weight factor, representing the probability density $P_i(\delta)$ of different sizes in the partition function $X_q(\delta)$, whose proportion can be changed.

The q-order multifractal dimension D_q of the sequence $x(t)$ can be solved by the following formula [30]:

$$D_q = \begin{cases} \frac{1}{q-1}\lim\limits_{\delta\to 0}\frac{\ln\sum P_i^q(\delta)}{\ln\delta} & (q \neq 1) \\ \lim\limits_{\delta\to 0}\frac{\sum P_i^q(\delta)\ln P_i^q(\delta)}{\ln\delta} & (q = 1) \end{cases} \tag{8}$$

The curve composed of multifractal dimension D_q and weight factor q is the generalized fractal dimension curve of sequence $x(t)$. The greater the deviation between multifractal dimension D_q and 1, the greater the volatility of data and the stronger the multifractal characteristics.

Singularity constant α and the subset fractal dimension $f(\alpha)$ can be calculated by the following formula [31].

$$\alpha = \frac{\mathrm{d}[\tau(q)]}{\mathrm{d}q} = \frac{\mathrm{d}\left[\lim\limits_{\delta\to 0}\frac{\ln X_q(\delta)}{\ln\delta}\right]}{\mathrm{d}q} \tag{9}$$

$$f(\alpha) = \alpha q - \tau(q) = \alpha q - \lim_{\delta\to 0}\frac{\ln X_q(\delta)}{\ln\delta} \tag{10}$$

The curve composed by α and $f(\alpha)$ is the multifractal spectrum of the sequence $x(t)$, which can reflect the nature of uneven distribution in the sequence $x(t)$. According to the multifractal characteristics [32], the subset represented by α_{min} corresponds to small signal, the subset represented by α_{max} corresponds to large signal, and multifractal spectrum width $\Delta\alpha = \alpha_{\max} - \alpha_{\min}$ describes the non-uniformity of signal distribution on the sequence $x(t)$ in the fractal structure, the larger $\Delta\alpha$ is, the greater the difference in signal distribution is,

and the more intense the fluctuation is. Let $\Delta f(\alpha) = f(\alpha_{\max}) - f(\alpha_{\min})$, then Δf represents the ratio of the number of signals in the correlation sequence subset at the maximum and minimum, the smaller $\Delta f(\alpha)$ is, the larger the proportion of large signal in the sequence is, and vice versa.

Through the above formula, the multiple information dimensions and multifractal spectra of EMR and AE excited by coal splitting failure can be obtained. By using the above characteristics to describe the nonlinear characteristics of acoustic and electrical signals, the relationship and difference between them can be compared.

3. Analysis of Experimental Results

3.1. Analysis of Coal Failure Process

The typical characteristics of the load, EMR and AE signals during the loading process are obtained by splitting loading the coal samples, as shown in Figure 2. It can be seen from the figure that the crack propagation of coal splitting failure is relatively simple, there is almost no pulse signal generated by EMR and AE, which indicates that before the splitting failure of coal, the internal damage is little and there is no macroscopic crack. Although the change of load is relatively uniform in the early stage of loading, it is still not an absolute linear change. Especially in the first 5 s of loading, the load curve fluctuates, related to the heterogeneity of coal.

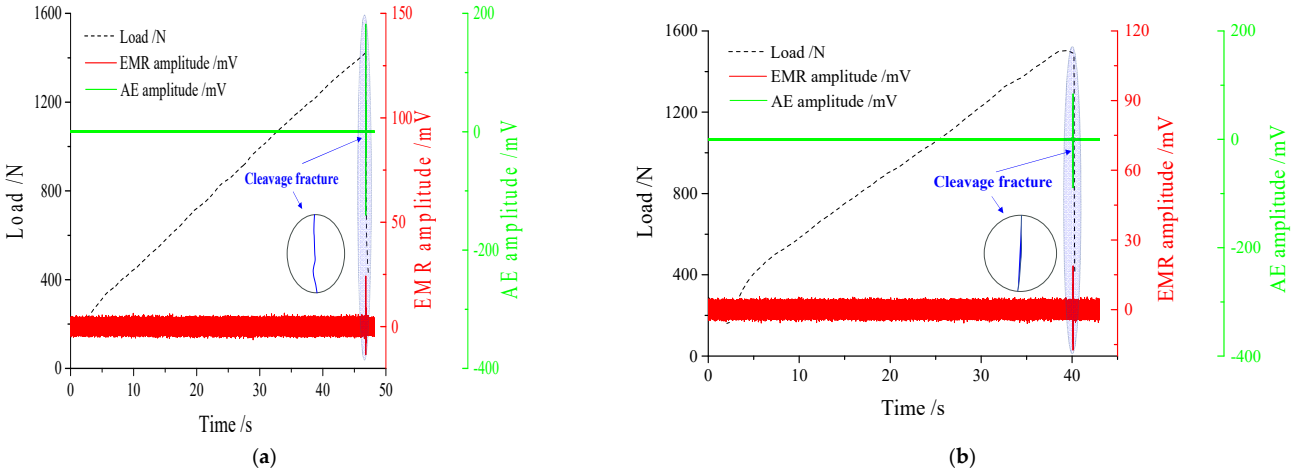

Figure 2. EMR and AE test results of coal splitting failure (**a**) Sample 1, (**b**) Sample 2.

At the later stage of loading, when the load reaches the peak value of the coal sample, the coal samples break suddenly, and a significant macro crack appears in the center of the sample, passing through the whole sample. At this time, the load curve decreased significantly. Sample 1 broke at 46.834 s, the load decreased from 1424.396 N to 660.791 N within 0.078 s, and the reduction rate was 9790 N/s. Sample 2 broke at 40.220 s, the load decreased from 1487.713 N to 397.354 N within 0.080 s, and the reduction rate was 13,629 N/s. When the sample is cracked, the EMR and AE signals respond well. The EMR amplitude of sample 1 reaches 24.2 mV and the AE amplitude reaches 182.0 mV. The EMR amplitude of sample 2 reaches 18.84 mV and the AE amplitude reaches 83.80 mV. It is worth noting that due to the complexity of the original internal micro-pores and micro-fissures and the heterogeneity of the coal samples. However, splitting can destroy the coal sample along the main crack, the crack surface is very rough, and the macro main fracture crack is not quite straight, but has a certain deflection. Therefore, we have reason to believe that the complexity of coal fracture will be more serious at the micro-scale of fracture.

In Figure 2, although the tested signal is filtered, the impact of environmental EMR on the test results is still greater than that of AE. Fortunately, in the later analysis, we found that the intensity of the EMR signal excited by coal fracture is much greater than environmental interference.

3.2. Waveform Characteristics of EMR and AE in Coal Failure

Figure 3 shows the typical EMR and AE waveforms corresponding to the main rupture in Figure 2. It can be seen that EMR and AE signals have good consistency in time, and the shock initiation time of waveform is consistent, which can be considered to be caused by the same fracture event of the sample. Figure 3 presents that the fluctuation range of EMR intensity of sample 1 is [−13.0 mV, 24.2 mV], the fluctuation range of AE intensity is [−141.0 mV, 182.0 mV], the fluctuation range of EMR intensity of sample 2 is [−17.21 mV, 18.84 mV], the fluctuation range of AE intensity is [−89.76 mV, 83.8 mV], and the amplitudes of AE and EMR signals are not proportional. It shows that there is not only a simple positive correlation between them.

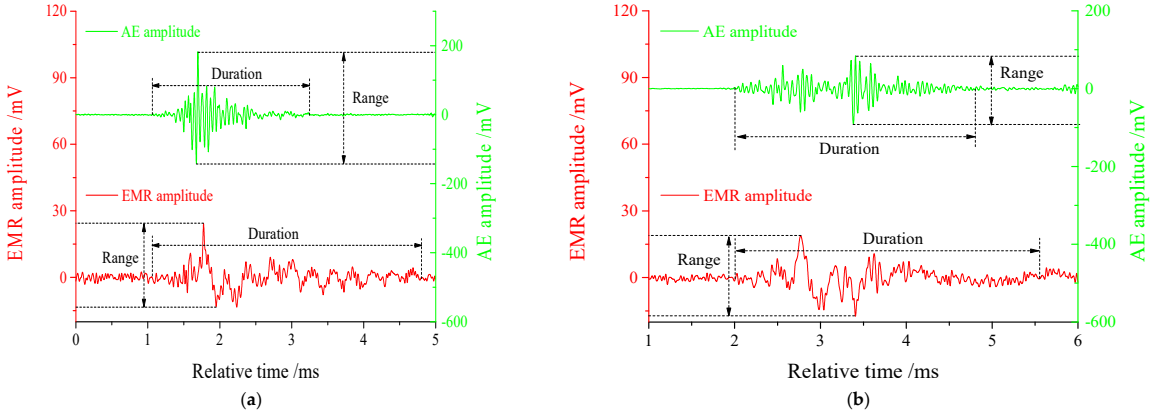

Figure 3. EMR and AE waveform of coal splitting failure (**a**) Sample 1, (**b**) Sample 2.

Although the initiation time of EMR and AE are the same in the two experiments, their end time differs, so their signal duration differs. The duration of the EMR waveform of sample 1 and sample 2 are 3.75 ms and 3.55 ms, respectively, while the duration of the AE waveform is 2.19 ms and 2.79 ms respectively. It shows that the duration of electromagnetic wave excited by the coal fracture event is longer than that of mechanical wave.

Figure 4 shows the frequency spectrum of EMR and AE waveform of the main fracture event of coal in Figure 3. It can be seen from the figure that the main frequency bands of EMR and the AE of the main fracture event are concentrated in the same range from 0 to 49 kHz. However, there are great differences in the distribution of the two signals at different frequencies. The dominant frequencies of EMR in the two tests are 3.404 kHz and 0.667 kHz respectively. In contrast, the dominant frequencies of AE are 17.419 kHz and 16.332 kHz, respectively, indicating that the frequency of AE is higher than that of EMR and the AE signal fluctuates more violently.

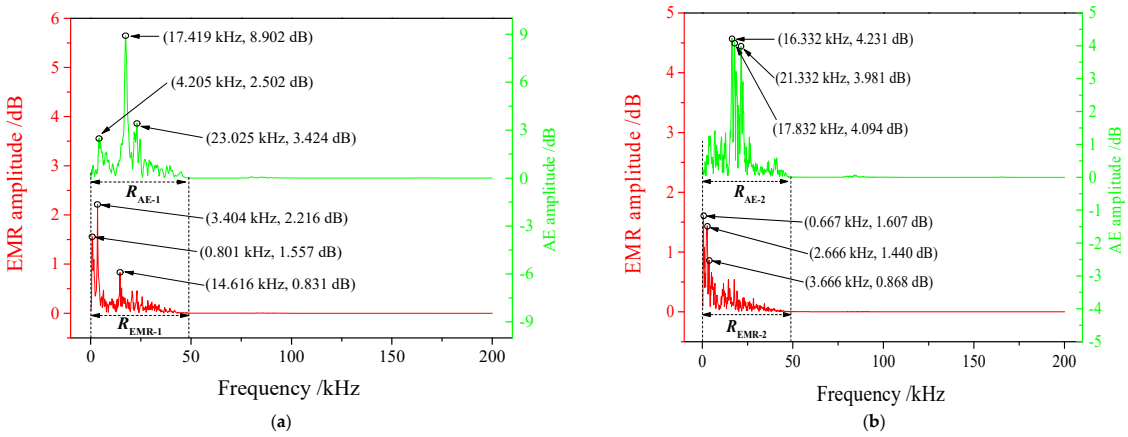

Figure 4. Frequency spectra of EMR and AE waveform of coal splitting failure (**a**) Sample 1, (**b**) Sample 2.

From the above analysis on the EMR and AE signals characteristics of coal splitting failure, it can be seen that both EMR and AE signals are generated by the same fracture event of coal, with the same starting time and main signal frequency band. However, both are not directly related, the intensity is not a simple positive correlation, and each shows different characteristics. The duration of EMR is longer than AE, but AE fluctuates more violently than EMR.

4. Fine Characteristics of the EMR and AE Waveform of Coal Splitting Failure Based on Hilbert-H Transform

4.1. IMF Characteristics of EMR and AE Waveform

Taking the EMR and AE waveform excited by the splitting failure of sample 1 as an example, the EMR and AE waveform signals are automatically decomposed into IMF components of different orders through empirical mode decomposition, and drawn from IMF1 to IMF8, respectively, according to the frequency from high to low, as shown in Figure 5.

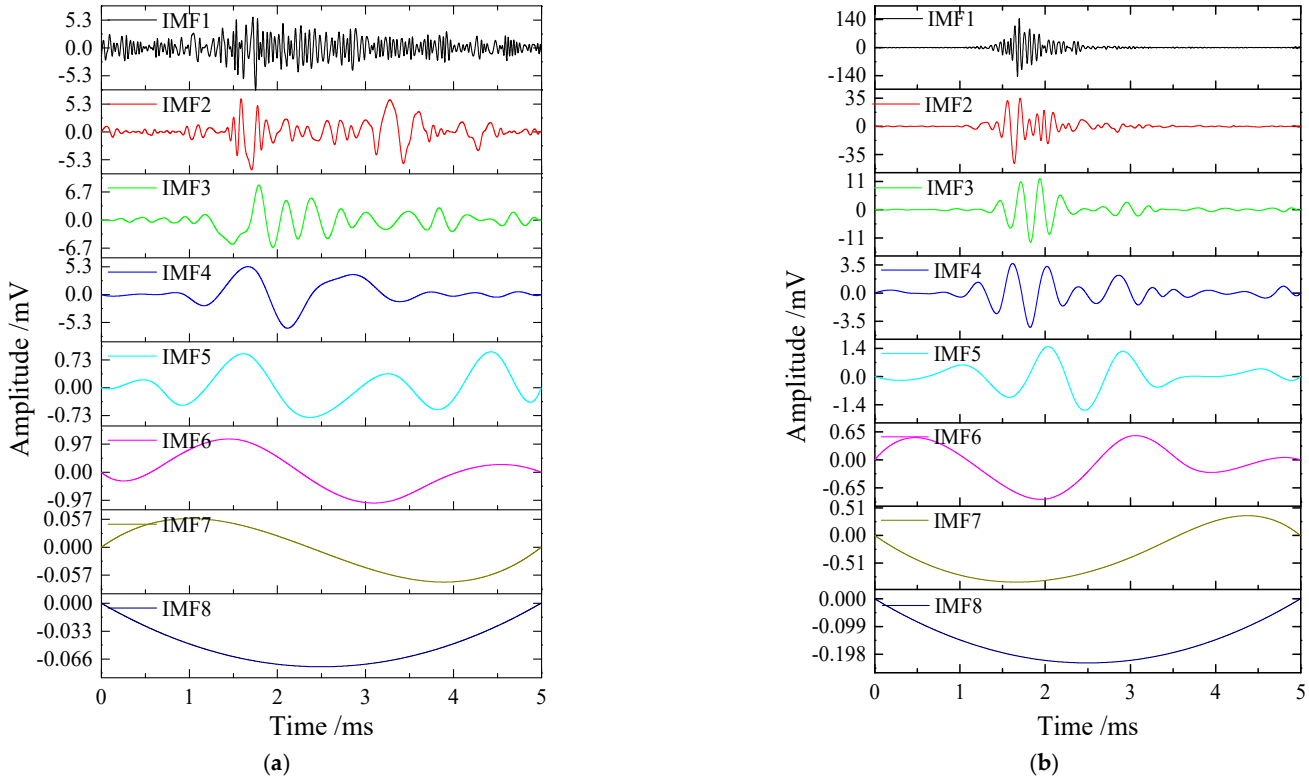

Figure 5. EMD components of EMR (**a**) and AE (**b**) waveform induced by splitting failure.

Figure 5 shows that the EMR waveform and AE waveform excited by coal splitting failure can be decomposed into different IMF components. With the increase of IMF order, the average frequency basically decreases gradually. The amplitude evolution law of the IMF component is obtained after statistics, as shown in Figure 6. It can be seen that the energy of the EMR waveform increases first and then decreases. The energy is mainly concentrated in IMF1~IMF4 order components, and the energy value is relatively evenly distributed in these four orders. In contrast, the energy of the AE waveform is unevenly distributed in each order, showing a monotonic decreasing trend. It mainly focuses on the IMF1 order components. Therefore, in applying mine safety monitoring, we should focus on the IMF1~IMF4 for EMR, while AE mainly focuses on the IMF1.

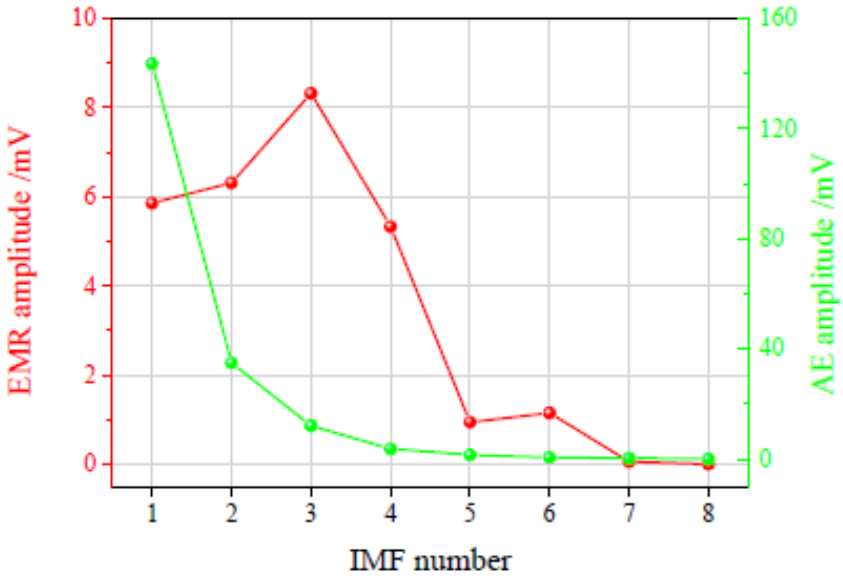

Figure 6. The maximum amplitude of different components of EMD of EMR and AE.

4.2. EMR and AE Waveform Hilbert Instantaneous Energy Spectrum

The Hilbert instantaneous energy spectrum of coal splitting EMR and AE waveform is shown in Figure 7. It can be seen from the figure that the EMR signal energy increases rapidly from 0.86 ms, reaches the maximum at 1.74 ms, then decreases gradually, returns to the noise level at 4.96 ms, and the energy is concentrated in the time range of 4.10 ms at the center of the waveform. The energy of the AE signal increases rapidly from 1.00 ms, reaches the maximum value at 1.69 ms, and then decreases rapidly. It returns to the noise level at 3.30 ms, and the energy is concentrated in the time range of 2.30 ms in the waveform center. The difference between the starting time of the EMR and AE signal is 0.14 ms, the difference between the occurrence time of energy peak is 0.05 ms, and the difference between the energy concentration range is 1.80 ms, which indicates that both EMR and AE should be closely related to the fracture event and its intensity. In this regard, they are consistent, that is, their origins are the same, and the difference in duration indicates that they are excited in different forms. When the coal is broken, the vibration duration is shorter, while the electromagnetic induction time is longer, which may be due to the longer time required for charge neutralization.

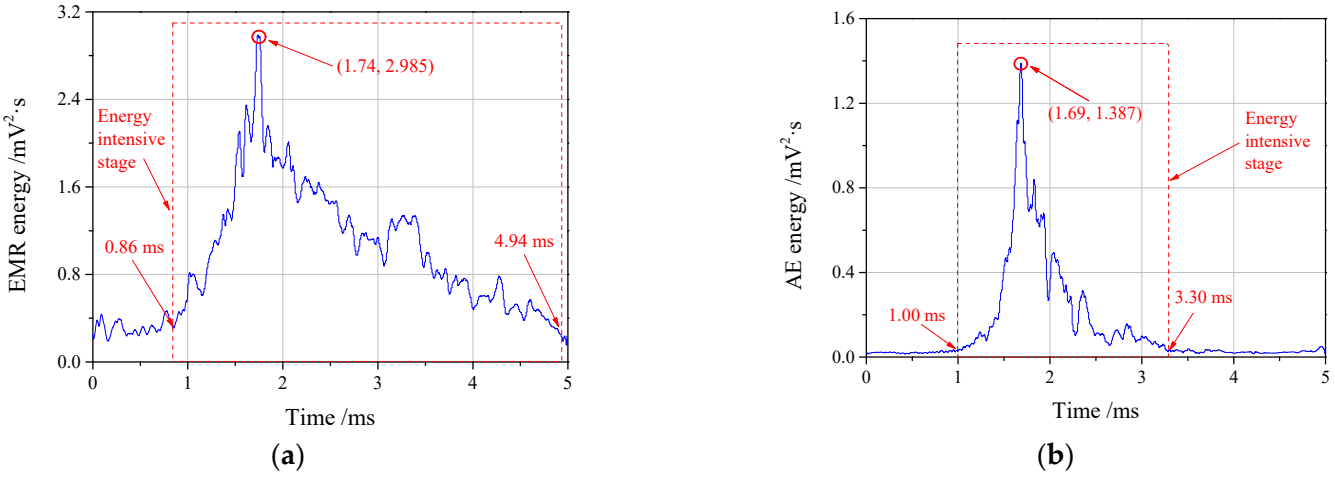

Figure 7. Hilbert instantaneous energy spectrum of EMR (**a**) and AE (**b**) waveform from Figure 3, Sample 1.

Hilbert instantaneous energy provides an energy characterization method in the time domain for acoustic and electrical signals, breaks through the limitations of energy characterization of traditional the EMR waveform in the whole process or frequency domain, and can provide an important basis for the study of the mechanism of EMR generation.

4.3. Three Dimensional Hilbert SPECTRUM of EMR and AE Waveform

The energy frequency–time three-dimensional Hilbert energy spectrum of EMR and the AE waveform of the coal splitting failure is shown in Figure 8. The abscissa represents time, and the ordinate represents the instantaneous frequency of the signal. The vertical coordinate and color correspond to the instantaneous energy value of the signal. It can be seen from the figure that the energy distribution of the EMR waveform excited by coal splitting failure is 1~5 ms, and the frequency is mainly distributed in the low-frequency band within 49 kHz. The signal-to-noise ratio of the EMR waveform is low and the frequency band is relatively wide. The signal-to-noise ratio of the AE waveform is higher than EMR, and the energy distribution of the AE waveform is mainly distributed in 1~3 ms. The frequency is mainly distributed in the low-frequency band within 49 kHz, but its dominant frequency is slightly higher than EMR, and the frequency band in which energy is concentrated is narrower than EMR. The three-dimensional Hilbert energy spectrum intuitively shows the distribution of EMR and AE waveforms at different times, frequencies and energy. It is found that they have great differences in instantaneous frequency and instantaneous energy. This method might be used to analyze and identify EMR and AE signals in different failure types and periods in other rock mechanics experiments.

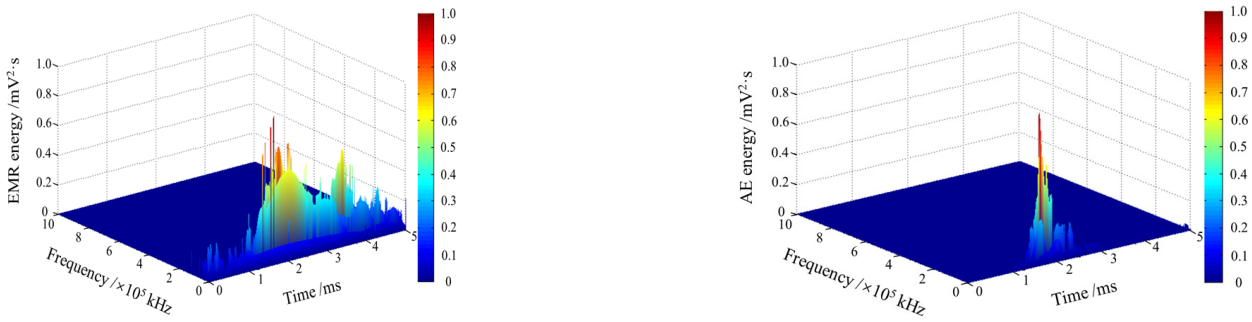

(**a**) (**b**)

Figure 8. Three-dimensional of Hilbert energy spectrum of EMR (**a**) and AE (**b**) waveform.

The research results on the time-frequency fine characteristics of EMR and AE signals excited by coal splitting failure show that they have great differences in the characteristics of frequency and instantaneous energy. EMR and AE should be closely related to the fracture process and fracture intensity, and have the same excitation source, but the excited forms are different. Compared with AE, the dominant frequency of EMR is lower, the frequency band is wider, the waveform duration is longer, and the energy distribution is more dispersed in the duration.

5. Fractal Characteristics of Acoustic and Electrical Signals of Coal Splitting Failure

5.1. Generalized Information Dimension of Acoustic Signals

Fractal feature analysis is an effective means for signal nonlinear feature analysis. In order to study the nonlinear characteristics of the EMR and AE signals of coal splitting failure, the data from initiation to the end (within the duration) of EMR signal 1 and AE signal 1 in Figure 3 are intercepted, and their fractal characteristics are analyzed by using the method described in Section 2.3.2.

The partition functions of EMR and AE waveforms are obtained by Formula (7), as shown in Figure 9. It can be seen from the figure that no partition function curves maintain the desired linear attenuation and converge at $\ln\delta = 0$, indicating that the two

waveforms have high scale invariance and belong to the category of multifractal. Therefore, the multifractal method can be used to study the difference and relationship between them.

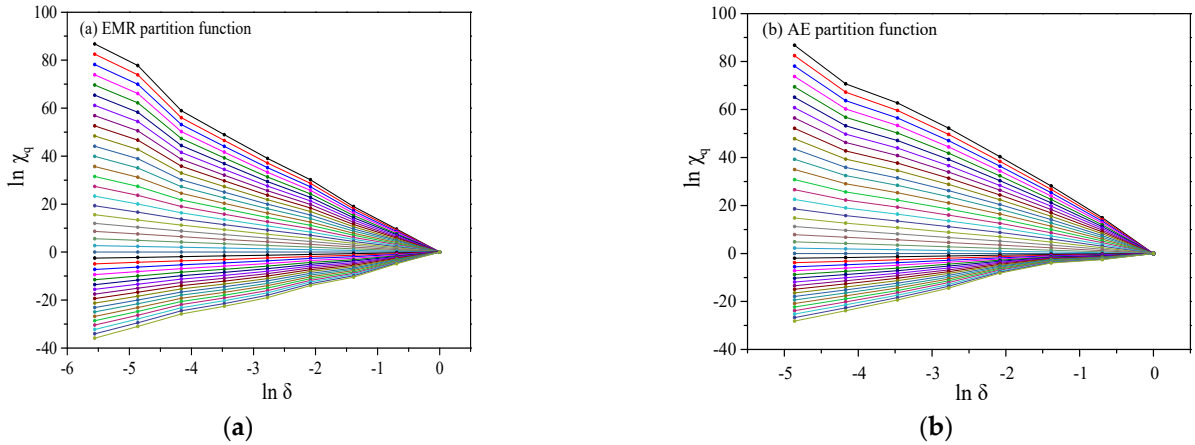

Figure 9. The partition function of EMR (**a**) and AE (**b**).

According to the calculation method of formula (8), the information dimension of the EMR and AE waveforms of coal splitting failure is calculated as shown in Figure 10. It can be seen from the figure that the multifractal dimensionality D_q of both EMR and AE induced by coal splitting failure is a monotonic decreasing function of q. If a column of data has multifractal characteristics, the multifractal dimensional value D_{qmax} corresponding to the minimum value q_{min} of the weight factor can reflect the non-uniformity and multifractal characteristics of the data. The greater the maximum value of D_q *is*, the more uneven the data is, and the stronger the multifractal characteristics are. In Figure 10, the D_{qmax} of EMR is 1.5611 and that of AE is 1.4177, indicating that the non-uniformity of EMR is higher than that of AE, and the multifractal characteristics are more obvious.

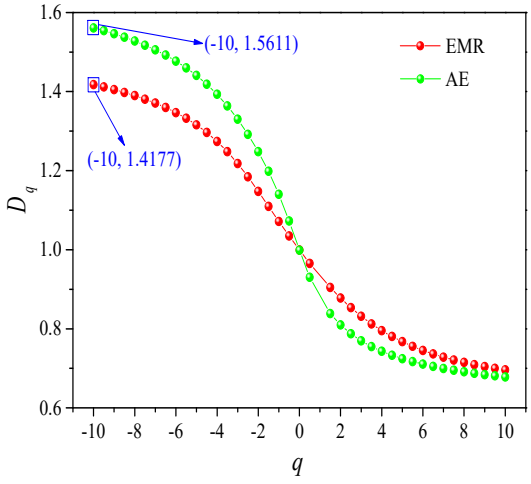

Figure 10. The generalized information dimension of EMR and AE waveforms of coal splitting failure.

This result is consistent with the generation mechanism of the EMR and AE signals during coal fracture. The fracture process of coal is complicated, which leads to the nonlinearity of EMR and AE generated by the fracture event. According to the previous research results, the duration of the EMR signal is greater than that of the AE signal, indicating that the EMR contains the information of coal fracture events and the characteristics of charge dissipation after a fracture. This ultimately shows more complicated nonlinear characteristics than the AE. Therefore, it is reasonable to believe that the D_{qmax} size of EMR and AE waveform can reflect the information of coal rock fracture events.

5.2. Multifractal Spectrum of Electromagnetic Signal

According to the calculation method of Formulas (9) and (10), the multifractal spectrums of EMR and AE waveforms are obtained, as shown in Figure 11. It can be seen from the figure that the multifractal spectrums of EMR and AE induced by coal splitting failure are similar, showing a "∩" shape, both of them show good multifractal characteristics. The fractal dimension of the subset of waveform data series $f(\alpha)$ shows an increasing and then decreasing pattern with the increase of the singularity constant α, which shows that they are similar in fractal characteristics.

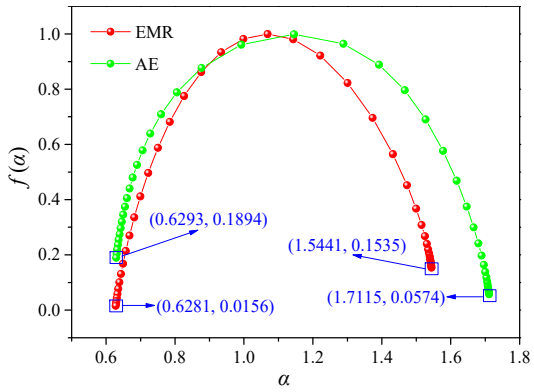

Figure 11. The multifractal spectrum of EMR and AE waveforms of coal splitting failure.

The difference is that the minimum and maximum values of the singularity constant α and the spectral width $\Delta\alpha$ are not the same for EMR and AE. The α_{min}, α_{max}, and $\Delta\alpha$ of EMR are 0.6281, 1.5441 and 0.9160, respectively, while the α_{min}, $\alpha_{max,}$ and $\Delta\alpha$ of AE are 0.6293, 1.7115 and 1.0822, respectively, which also verifies that they are not the same signal. The spectral width $\Delta\alpha$ characterizes the degree of inhomogeneity of the signal distribution on the fractal structure. The results show that the volatility of AE signal is greater than that of EMR, which is consistent with Figure 3, in which AE signal 1 increases rapidly after vibration initiation and decreases rapidly after reaching the peak value. The fluctuation amplitude is 323 mV in the duration of 2.19 ms, and the volatility of the signal is 147.49 mV/ms, while the EMR signal 1 fluctuates at 37.2 mV in 3.75 s. The fluctuation of signal duration is 9.92 mV/ms, which is far lower than that of AE. Meanwhile, the interval length of fluctuation of AE signal 2 in Figure 3 is 62.2 mV/ms, while the interval length of fluctuation of EMR signal 2 is 10.15 mV/ms. The laws of the two groups of signals are consistent, that is, the interval length of fluctuation of AE signal generated by coal splitting is greater than that of EMR.

In addition, the fractal dimension $f(\alpha)$ of the sequence subset of EMR and AE have different $f(\alpha)$ dimensions. The $f(\alpha_{min})$, $f(\alpha_{max})$ and $\Delta f(\alpha)$ of EMR are 0.0156, 0.0574 and 0.0418, respectively. The $f(\alpha_{min})$, $f(\alpha_{max})$ and $\Delta f(\alpha)$ of AE are 0.1894, 0.0574 and -0.1320, respectively, where Δf represents the ratio of the number of signals in the correlation sequence subset at the maximum and minimum, $\Delta f(\alpha)$ is smaller, indicating that the proportion of large signals in the sequence is larger, and vice versa. The $\Delta f(\alpha)$ of EMR is positive and greater than that of AE, which indicates that in the EMR waveform within the duration (from shock initiation to attenuation to calm), the signal distribution is relatively uniform and the proportion of large signal is less. In contrast, the AE signal distribution is uneven. After the appearance of fracture, the signal rises rapidly to a higher level, and the proportion of strong signals is more in the duration.

The research results in this section show that EMR shows more complicated nonlinear characteristics than AE, and the information of EMR contained not only the coal failure process, but also the late charge dissipation process, which is likely to be crack closure or complete separation of the walls. Further research is expected to identify the scale and even location of the fracture, which has a certain value for the study of rock mechanics.

It should be noted that in this experiment, the maximum frequency of EMR and AE signals is lower than 50 kHz, and their sampling frequency is 2 MHz, which is more than 40 times the maximum signal frequency. Therefore, in the process of A/D conversion and data processing, the timing characteristics, frequency characteristics and fractal characteristics of signals are stable, ultimately supporting the reliability of the analyzed results.

6. Discussion of the Mechanism of EMR Generation during Coal Splitting

The crack propagation diagram of splitting failure is shown in Figure 12. The coal sample breaks under the Brazilian Splitting, and then the crack expands downward along the vertical direction under tensile stress. According to the previous research results on coal micro morphology and fracture characteristics [33,34], due to the heterogeneity of coal, the direction and size of the propagation speed $\vec{v_e}$ are variable, and its size order is at the level of 10^2 m/s [35]. During crack expansion, due to the tip effect, charge separation occurs in the area around the crack, negative charges are accumulated in front of the crack, and positive charges are accumulated on the crack wall. In this charge separation process, the electromagnetic induction field will be excited.

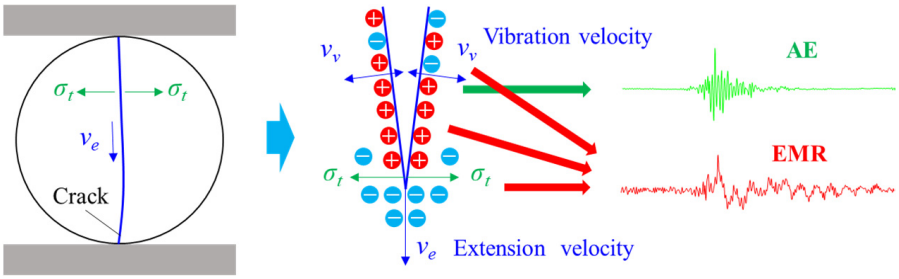

Figure 12. Schematic diagram of EMR and AE induced by crack propagation during coal splitting.

Since the moving direction of negative charge after charge separation is fixed (moving in front of the crack), the frequency f_{se} of the electromagnetic induction field excited by charge separation at the crack tip is low.

The crack propagation process will drive the crack wall to vibrate. Due to the limited space around the crack, the wall vibration is cyclic and has a certain frequency. In general, its frequency is between a few Hz and a few MHz. In this coal splitting process, the frequency is between approximately 0 and 49 kHz, consistent with the previous test results [36].

In addition, during the vibration of the crack wall, the positive charge around the crack moves with it, resulting in an electromagnetic induction field in the surrounding space. Due to the repulsion between the same polarity charges, the damping of charge motion is greater than that of wall vibration, resulting in a higher frequency attenuation. Therefore, the frequency f_{ew} of electromagnetic induction field excited by wall vibration should be lower than the frequency f_a of AE. It is consistent with the test results of this experiment.

After the crack propagation stops, the crack vibration stops gradually under the action of damping. The total time of crack vibration is the duration of AE in Figure 3. After that, because no new crack is generated, the separated charges around the original crack combine the positive and negative charges again under the action of electric field force, and the frequency f_{en} of the electromagnetic induction field excited by this process is also low.

To sum up, the frequency of EMR is lower than that of AE in each stage of coal fracture, which is the mechanism of low-frequency EMR in the process of coal fracture.

Since crack propagation and wall vibration are almost the same, the excitation start time of the EMR induction field and AE is the same in the above process analysis. The research results in Figure 3 also prove this, which shows that the sources of EMR and AE are the same, both from the coal crack surface. After the crack wall stops shaking, the AE intensity decreases to a low level, but the electromagnetic induction field excited by the charge neutralization process still exists for some time. Therefore, for the same rupture, the duration of EMR is longer than that of AE.

According to previous studies, the piezoelectric crystal inside the coal will induce an electromagnetic field during loading [26,37,38]. Therefore, in the whole process of loading, the intensity of EMR is difficult to reduce to a low level, and the signal-to-noise ratio of the EMR signal is poor, which is consistent with the results in Figure 3.

EMR of coal splitting failure has many sources, and the early stage of fracture is mainly due to the piezoelectric effect. In the process of crack propagation, there are both signals excited by charge separation and signals induced by crack wall vibration. The end of crack growth is mainly the signal of charge neutralization and excitation. This may be the reason why the complexity of EMR is greater than that of AE excited by the same fracture.

The non-linear nature of EMR signals is essentially the velocity variable motion of charge, and the reason for the velocity variable motion of the charge is the non-uniform distribution of charge around crack surface and the cracks complicated vibration during coal fracture.

7. Conclusions

In this paper, the fine nonlinear characteristics of EMR and the AE waveform of coal splitting failure are studied using the Hilbert-H transform and multifractal theories, and the correlation mechanism between EMR of coal splitting failure and crack propagation is revealed. The main conclusions are as follows:

(1) EMR and AE signals of coal splitting failure are related to crack propagation. Their initiation time is basically the same and the main signal concentration frequency band is the same (0~49 kHz), but their signal duration is different. The duration of electromagnetic wave excited during coal fracture is longer than the mechanical wave, and the main frequency of the AE signal is higher than EMR.

(2) The EMR energy of coal splitting failure is mainly concentrated in the IMF1~IMF4 order components of EMD decomposition, and the AE energy is mainly concentrated in the IMF1 order components. EMR and AE excited during splitting failure have the same excitation source, but different excitation modes.

(3) The results of the multifractal analysis show that in the duration of EMR of coal splitting failure, the signal distribution is relatively uniform, and the proportion of the large signal is lower. EMR shows more complicated multifractal characteristics than AE, and contains more information than AE.

(4) During coal splitting failure, AE is mainly generated in the process of wall vibration caused by crack propagation. At the same time, the generation of EMR includes piezoelectric effect, charge separation, free charge vibration, charge neutralization and other processes, which is more complicated than AE and has a relatively low frequency.

The research provides an effective method of analyzing signal characteristics of coal EMR and AE, breaking through the limitations of traditional characterization methods in the whole process or frequency domain, and can provide an important basis for the study of the mechanism of EMR generation.

Author Contributions: Conceptualization, L.Q. and D.S.; Methodology, L.Q.; Software, Y.Z.; Validation, Y.Z. and W.W.; Formal Analysis, Y.Z.; Investigation, Y.L.; Resources, Y.X.; Data Curation, X.H.; Writing-Original Draft Preparation, L.Q.; Writing-Review & Editing, Y.Z., M.W., S.Y. and Q.L.; Visualization, L.Q.; Supervision, D.S.; Project Administration, X.H.; Funding Acquisition, L.Q. and D.S. All authors have read and agreed to the published version of the manuscript.

Funding: This work was financially supported by the National Natural Science Foundation of China (52004016, 52174162, 51904019), the State Key Laboratory Cultivation Base for Gas Geology and Gas Control (Henan Polytechnic University) (WS2020B01), the Open Fund Project of Shaanxi Key Laboratory of Prevention and Control Technology for Coal Mine Water Hazard (2021SKMS05), Science and Technology Support Plan Project of Guizhou Province ([2021]515).

Conflicts of Interest: The authors declare no conflict of interest.

References

1. Ma, Y.; Nie, B.; He, X.; Li, X.; Meng, J.; Song, D. Mechanism investigation on coal and gas outburst: An overview. *Int. J. Miner. Metall. Mater.* **2020**, *27*, 872–887. [CrossRef]
2. Bai, G.; Su, J.; Zhang, Z.; Lan, A.; Zhou, X.; Gao, F.; Zhou, J. Effect of CO_2 injection on CH_4 desorption rate in poor permeability coal seams: An experimental study. *Energy* **2022**, *238*, 121674. [CrossRef]
3. Feng, J.; Wang, E.; Ding, H.; Huang, Q.; Chen, X. Deterministic seismic hazard assessment of coal fractures in underground coal mine: A case study. *Soil Dyn. Earthq. Eng.* **2020**, *129*, 105921–105931. [CrossRef]
4. Liao, Z.; Liu, X.; Song, D.; He, X.; Nie, B.; Yang, T.; Wang, L. Micro-structural damage to coal induced by liquid CO_2 phase change fracturing. *Nat. Resour. Res.* **2021**, *30*, 1613–1627. [CrossRef]
5. Xia, Y.; Liu, B.; Zhang, C.; Liu, N.; Zhou, H.; Chen, J.; Tang, C.; Gao, Y.; Zhao, D.; Meng, Q. Investigations of mechanical and failure properties of 3D printed columnar jointed rock mass under true triaxial compression with one free face. *Geomech. Geophys. Geo-Energy Geo-Resour.* **2022**, *8*, 26. [CrossRef]
6. Qiu, L.; Song, D.; Li, Z.; Liu, B.; Liu, J. Research on AE and EMR response law of the driving face passing through the fault. *Saf. Sci.* **2019**, *17*, 184–193. [CrossRef]
7. Song, D.; Wang, E.; Song, X.; Jin, P.; Qiu, L. Changes in frequency of electromagnetic radiation from Loaded coal. *Rock Mech. Rock Eng.* **2016**, *49*, 291–302. [CrossRef]
8. He, M.; Miao, J.; Feng, J. Rock burst process of limestone and its acoustic emission characteristics under true-triaxial unloading conditions. *Int. J. Rock Mech. Min. Sci.* **2010**, *47*, 286–298. [CrossRef]
9. Kong, X.; Li, S.; Wang, E.; Wang, X.; Zhou, Y.; Ji, P.; Shuang, H.; Li, S.; Wei, Z. Experimental and numerical investigations on dynamic mechanical responses and failure process of gas-bearing coal under impact load. *Soil Dyn. Earthq. Eng.* **2021**, *142*, 106579. [CrossRef]
10. Chen, Z.; Li, T.; Chen, G.; Zhang, H. Experimental study of acoustic emission characteristics of sandstone under hydro-mechanical coupling action. *Rock Soil Mech.* **2014**, *35*, 2815–2822.
11. Qiu, L.; Wang, E.; Song, D.; Liu, Z.; Shen, R.; Xu, Z. Measurement of the stress field of a tunnel through its rock EMR. *J. Geophys. Eng.* **2017**, *14*, 949–959. [CrossRef]
12. Frid, V.; Vozoff, K. Electromagnetic radiation induced by mining rock failure. *Int. J. Coal Geol.* **2005**, *64*, 57–65. [CrossRef]
13. He, X.; Dou, L.; Mu, Z.; Gong, S.; Cao, A. Continuous monitoring and warning theory and technology of rock burst dynamic disaster of coal. *J China Coal Soc.* **2014**, *39*, 1485–1491.
14. Lichtenberger, M. Underground measurements of electromagnetic radiation related to stress-induced fractures in the Odenwald Mountains (Germany). *Pure Appl. Geophys.* **2006**, *163*, 1661–1677. [CrossRef]
15. Qiu, L.; Li, Z.; Wang, E.; Liu, Z.; Ou, J.; Li, X.; Ali, M.; Zhang, Y.; Xia, S. Characteristics and precursor information of electromagnetic signals of mining-induced coal and gas outburst. *J. Loss Prev. Process Ind.* **2018**, *54*, 206–215. [CrossRef]
16. Gade, S.; Alaca, B.; Sause, M. Determination of Crack Surface Orientation in Carbon Fibre Reinforced Polymers by Measuring Electromagnetic Emission. *J. Nondestruct. Eval.* **2017**, *36*, 21. [CrossRef]
17. Greiling, R.; Obermeyer, H. Natural electromagnetic radiation (EMR) and its application in structural geology and neotectonics. *J. Geol. Soc. India* **2010**, *75*, 278–288. [CrossRef]
18. Ogawa, T.; Oike, K. Electromagnetic radiation from rocks. *J. Geophys. Res.* **1985**, *90*, 6245–6249. [CrossRef]
19. Cress, G.; Brady, B.; Rowell, G. Sources of electromagnetic radiation from fracture of rock samples in the laboratory. *Geophys. Res. Lett.* **1987**, *14*, 331–334. [CrossRef]
20. Zhu, Y.; Luo, X.; Guo, Z.; Zhao, Z.; Zhu, Z. Study on the mechanism of electromagnetic radiation during rock fracture. *Chin. J. Geophys.* **1991**, *34*, 594–601.
21. Rabinovitch, A.; Frid, V.; Bahat, D. Surface oscillations-A possible source of fracture induced electromagnetic radiation. *Tectonophysics* **2007**, *431*, 15–21. [CrossRef]
22. Pan, Y.; Luo, H.; Tang, Z.; Li, Z.; Zhao, Y. Study on charge induction law of tensile instability failure of coal rock mass. *Chin. J. Rock Mech. Eng.* **2013**, *32*, 1297–1303.
23. Han, J.; Huang, S.; Zhao, W.; Wang, S. Stress excited electrical dipole model for electromagnetic emission induced in fractured rock. *Int. J. Appl. Electromagn. Mech.* **2016**, *52*, 1023–1034. [CrossRef]
24. Li, Z.; He, S.; Song, D.; He, X.; Dou, L.; Chen, J.; Liu, X.; Feng, P. Microseismic temporal-spatial precursory characteristics and early warning method of rockburst in steeply inclined and extremely thick coal seam. *Energies* **2021**, *14*, 1186. [CrossRef]
25. Yoshida, S.; Ogawa, T. Electromagnetic emissions from dry and wet granite associated with acoustic emissions. *J. Geophys. Res. Solid Earth* **2004**, *109*, B09204. [CrossRef]
26. Wang, E.; He, X.; Li, Z.; Zhao, E. *Electromagnetic Radiation Technology of Coal and Rock and Its Application*; Science Press: Beijing, China, 2009.
27. Sa, Z.; He, X.; Wang, E.; Yu, G. An experimental study of the electromagnetic emission memory effect during the deformation and fracture of coal or rock. *Chin. J. Geophys.* **2005**, *48*, 379–385. [CrossRef]
28. Zhang, X.; He, M.; Wang, H. Study on the signal characteristics of electromagnetic emission during rock fracture. *Comput. Tech. Geophys. Geochem. Explor.* **2019**, *41*, 469–475.
29. Huang, N.; Shen, Z.; Long, S.; Wu, M.; Shih, S.; Zheng, Q.; Yen, N.; Tung, C.; Liu, H. The empirical mode decomposition and the Hilbert spectrum for nonlinear and non-stationary time series analysis. *Proc. Math. Phys. Eng. Sci.* **1998**, *454*, 903–995. [CrossRef]

30. Qiu, L.; Song, D.; He, X.; Wang, E.; Li, Z.; Yin, S.; Wei, M.; Liu, Y. Multifractal of electromagnetic waveform and spectrum about coal rock samples subjected to uniaxial compression. *Fractals* **2020**, *28*, 2050061. [CrossRef]
31. Li, X.; Li, Z.; Wang, E.; Liang, Y.; Li, B.; Chen, P.; Liu, Y. Pattern recognition of mine microseismic (MS) and blasting events based on wave fractal features. *Fractals* **2018**, *26*, 1850029. [CrossRef]
32. Feng, J.; Wang, E.; Huang, Q.; Ding, H.; Ma, Y. Study on coal fractography under dynamic impact loading based on multifractal method. *Fractals* **2020**, *28*, 2050006. [CrossRef]
33. Shen, R.; Qiu, L.; Zhao, E.; Han, X.; Li, H.; Hou, Z.; Zhang, X. Experimental study on frequency and amplitude characteristics of acoustic emission during the fracturing process of coal under the action of water. *Saf. Sci.* **2019**, *117*, 320–329. [CrossRef]
34. Si, L.; Wei, J.; Xi, Y.; Wang, H.; Wen, Z.; Li Bo Zhang, H. The influence of long-time water intrusion on the mineral and pore structure of coal. *Fuel* **2021**, *290*, 119848. [CrossRef]
35. Zhao, Y.; Sun, Z.; Song, H.; Zhao, S. Crack propagation law of mode I dynamic fracture of coal: Experiment and numerical simulation. *J. China Coal Soc.* **2020**, *45*, 3961–3972.
36. Qiu, L.; Liu, Z.; Wang, E.; He, X.; Feng, J.; Li, B. Early-warning of rock burst in coal mine by low-frequency electromagnetic radiation. *Eng. Geol.* **2020**, *279*, 105755. [CrossRef]
37. Nitsan, U. Electromagnetic emission accompanying fracture of quartz-bearing rocks. *Geophys. Res. Lett.* **1977**, *4*, 333–336. [CrossRef]
38. Russell, R.D.; Maxwell, M.; Butler, K.E.; Kepic, A.W. Electromagnetic responses from seismically excited targets A: Piezoelectric phenomena at Humboldt, Australia. *Explor. Geophys.* **1992**, *23*, 281–285. [CrossRef]